Contents lists available at SCCE

Journal of Soft Computing in Civil Engineering

Journal homepage: www.jsoftcivil.com

Flexural Capacity Prediction of RC Beams Strengthened in Terms of NSM System Using Soft Computing

Amin Raeisi [1]; Mohammad Kazem Sharbatdar [2]; Hosein Naderpour [2]; Pouyan Fakharian [3*]

1. M.Sc. Graduated, Faculty of Civil Engineering, Semnan University, Semnan, Iran
2. Professor, Faculty of Civil Engineering, Semnan University, Semnan, Iran
3. Ph.D. Candidate, Member of Scientific Society of Civil Engineering Students, Faculty of Civil Engineering, Semnan University, Semnan, Iran

Corresponding author: *pouyanfakharian@semnan.ac.ir*

https://doi.org/10.22115/SCCE.2024.429316.1761

ARTICLE INFO

Article history:
Received: 07 October 2023
Revised: 25 December 2023
Accepted: 01 January 2024

Keywords:
Machine learning;
Artificial neural network;
Predictive model;
Near-surface mounted (NSM);
FRP;
Flexural strength.

ABSTRACT

In recent years, there has been a notable increase in the application of near-surface mounted fiber-reinforced polymer (FRP) reinforcement in reinforced concrete structures. Nevertheless, there is a discernible disparity in the accessibility of accurate and customize measures for augmenting flexural strength through the use of near-surface mounted (NSM) reinforcement techniques. Although several basic models have been proposed to predict the flexural capacity achievable with this technology, established codes have not yet provided mathematical equations for this specific purpose. This study presents two separate methodologies with the objective of enhancing the development of suitable code provisions. In the first stage, A comprehensive and reliable database has been developed to leverage the predictive accuracy of neural networks in the computation of the flexural capacity of reinforced beams that utilize near-surface mounted reinforcement. Following this, the results obtained from the neural network are employed to construct a linear equation using the group method of data handling (GMDH) technique. The presented equation has been carefully formulated to produce a concise and simple mathematical expression that enables the determination of the flexural strength of a beam on the field. The evaluation of the accuracy and effectiveness of both the neural network and the suggested equation is conducted in accordance with the requirements specified in ACI 440.R2 for externally bonded reinforcements. The neural network's prediction has a mean absolute error of just 5% in comparison to the experimental results and the GMDH equations exhibit a noteworthy level of concurrence with the experimental outcomes, as they display a mean absolute error of 16%.

How to cite this article: Raeisi A, Sharbatdar MK, Naderpour H, Fakharian P. Flexural capacity prediction of RC beams strengthened in terms of NSM system using soft computing. J Soft Comput Civ Eng 2024;8(4): 1–26. https://doi.org/10.22115/scce.2024.429316.1761

2588-2872/ © 2024 The Authors. Published by Pouyan Press.
This is an open access article under the CC BY license (http://creativecommons.org/licenses/by/4.0/).

1. Introduction

The application of fiber reinforced polymer (FRP) reinforcement using the near surface mounted (NSM) technology has been increasingly prominent in enhancing the strength of reinforced concrete (RC) elements. The proposed methodology entails the creation of slots within the concrete cover, followed by the infusion of epoxy as a bonding agent, prior to the installation of the FRP reinforcement. Several research conducted over the past two decades have examined and contrasted the effectiveness of this strategy in relation to the externally bonded (EB) approach. The process of designing externally bonded FRP has been simplified due to the efforts of many international organizations, such as the American Concrete Institute (ACI) 440.2R-17 [1]. Nevertheless, according to research findings, de-bonding takes place at a low level of tension between the FRP and concrete surface, despite the broad use of the EB FRP approach. Therefore, this technique does not allow for the complete realization of the entire potential of FRP [2]. The advantages of the novel technology in comparison to the preceding (EB) method encompass enhanced safeguarding, a superior bond, heightened aesthetic appeal, improved surface preparation, and the possibility of securing attachment to adjacent components [3]. The enhancement of bond performance, in comparison to EB systems, is a crucial element in the construction of NSM-FRP systems [4]. Several elements linked to FRP, including the size of the bars, surface treatment, groove geometry, concrete properties, and adhesive used in the test setup, have been found to affect the bond between concrete and NSM FRP bars [5,6]. Over the course of the last ten years, there have been notable advancements in the near surface mounted technique, including the development of novel anchorage methods [7], and the utilization of cost-effective materials for manufacturing FRP bars at building sites [8]. The application of FRP systems to reinforce a bridge slab in the negative moment zone was first observed in northern Sweden during the 1940s, as documented by Asplund in 1949, in this particular process, the steel rods were incorporated into the concrete cover using cement mortar [9]. Four slabs were subjected to experimental reinforcement using an identical technique prior to the commencement of the strengthening procedure. Subsequently, these slabs were subjected to loading until failure occurred. In March 1949, an experiment was conducted where approximately 600 meters of steel bars were successfully bonded to the concrete cover. The results of this experiment provided evidence of the efficacy of this strategy. It is important to acknowledge that the establishment of a successful concrete cover bond in these projects presents a complex undertaking, as there may be instances where it is not feasible to pour concrete around the reinforcement bars [10]. A preliminary investigation on flexural strength of beam strengthened with NSM technique conducted at Lule University of Technology in 1996 assessed the initial rectangular FRP rods. In conjunction with a comprehensive investigation conducted by Lorenzis et al. [4], as well as the work of Hassan and Rizkalla et al [11] examined circular rods in 2001, the results demonstrated a significant enhancement in capacity, with improvements ranging from 25.7% to 44.3% compared to the control beam. However, it is evident that establishing a strong bond is crucial for the efficacy of this technique. The research undertaken by Nordin and Täljsten [12] revealed that the sawing of grooves for FRP reinforcement was only feasible when the steel reinforcement has an adequate level of "depth."

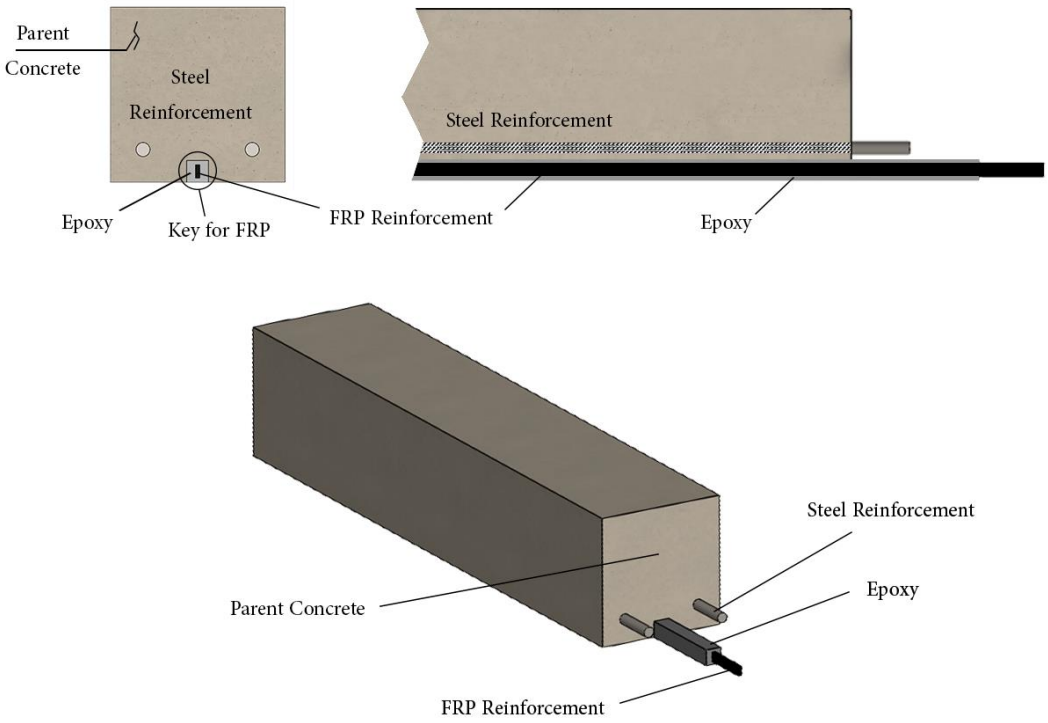

Fig. 1. Concrete member strengthened in flexure with NSM FRP.

It is imperative to acknowledge that the efficacy of this technique is contingent upon the thickness of the concrete cover, a parameter that exhibits variability based on the prevailing conditions encountered at the construction site. Hence, it may be inferred that outdoor structures, particularly bridges, may derive greater advantages from the suggested technique in comparison to inside ones, owing to their higher concrete coverage [9]. According to recent researches [13,14], examinations have shown that the use of NSM-FRP rods in reinforced concrete beams might potentially increase the Flexural Strength by up to 60.6%. This enhancement is dependent on the specific ratios of internal steel reinforcement and the subsequent behavior of the beams. The researchers investigated the bonding mechanism between NSM-FRP bars and its implications for flexural strengthening in concrete structures. The study stated earlier made predictions on the bond length limitations for each side of the beam's center line, with a clear span of 2500 millimeters. These limitations were estimated to be 150, 550, 800, and 1200 millimeters [15]. The results of the study indicate that the optimal development length for NSM-CFRP should not be reduced to a value less than 80 times the initial diameter, taking into account the specific properties of the materials and grooves employed. Conversely, the reinforced beams exhibited minimal reduction in ultimate load capacity when subjected to the modified epoxy adhesive. Furthermore, it was observed that the load capacity of the beams exhibited a modest improvement when the bond lengths exceeded 800 millimeters [16]. According to the results of the beam bond experiment conducted in reference [17], it was observed that longer rod bonds were associated with an augmented ultimate load capacity. Consequently, the resistance to splitting was enhanced through the process of widening the square grooves. In a previous study [18], the beams, which had a distinct span of 2800 millimeters, were reinforced by employing adhesive bonds with lengths measuring 2100, 2700, and 3000 millimeters. The utilization of

epoxy in the NSM system led to the breakdown of the system, resulting in the withdrawal of the rods and the detachment of the concrete cover from the end of the rods. In spite of the observed elongation of 3000 millimeters in the bond length, there was no discernible reduction in the maximum load deflection. Furthermore, the strength of the concrete had minimal influence on the load-carrying capacity of the reinforced beams [19].A subsequent investigation in this field examined the application of reinforced beams with less robust bonding, resulting in significant implications for failure modes such as the detachment of concrete or the extraction of CFRP rods. Furthermore, the cantilever beams that were reinforced and subjected to testing using a four-point flexure exhibited identical failure mechanisms, as reported in a previous study [20]. Based on the findings of a separate study [21], the utilization of CFRP strips as near-surface mounted (NSM) reinforcements, as opposed to EB-CFRP strips, resulted in a significant enhancement of the load-bearing capacity of reinforced beams, with an increase of 4.8 times. However, according to a recent study, the utilization of NSM CFRP strips to reinforce GFRP RC beams may eventually change the failure mode compared to the beams without reinforcement, resulting in more vulnerable failure modes such CFRP rupture or CFRP debonding [22].

2. Analytical approach

The Figure.2 shows the basic theoretical conditions of internal strain, stress, in the ultimate section that is under-reinforced with steel ($\rho_s < \rho_{sb}$), and it is strengthened by FRP. The essential assumptions for this condition are: throughout the cross section, the strain changes linearly, the section is not cracked at initial, there is a complete bond between the steel and FRP reinforcements and concrete, 0.003 is the level of concrete strain where the compression failure occurs, and in the compression area, the Whitney rectangular stress block considered a good substitution for the nonlinear distribution of stress at ultimate, and Finally, the behavior of steel is considered elastic-plastic in terms of stress-strain [6].

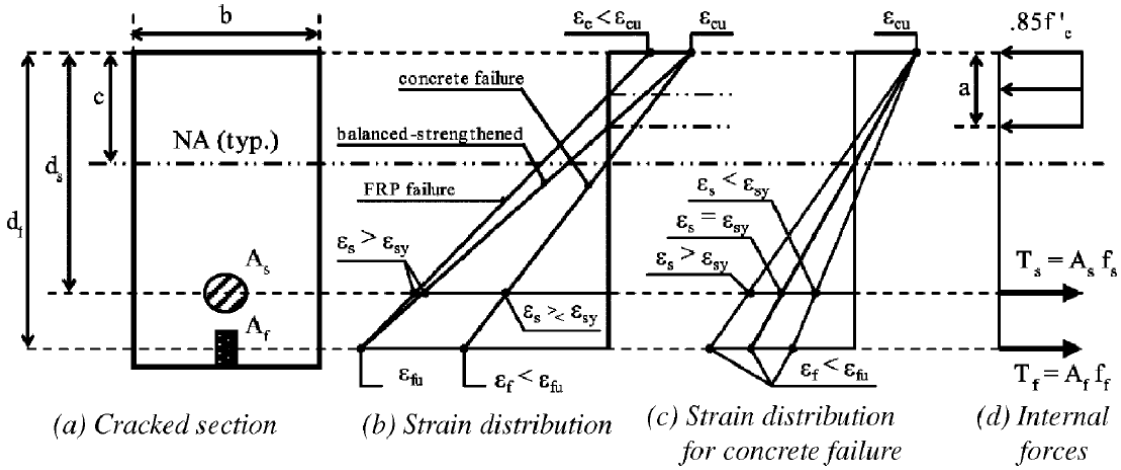

Fig. 2. Model analysis at ultimate [4].

Since the section is not cracked at first and $d_f > d_s$, the FRP strain ε_f will be almost higher than the steel strain ε_s. There is a dependency between the nominal flexural uncracked beam strength

M_n which is not fully reinforced with steel ($\rho_s < \rho_{sb}$) and strengthened with NSM-FRP and the FRP levels in comparison with FRP area of a well distributed strengthened strain (A_{fb}). In this context, balanced-strengthened is a representation of the FRP simultaneous tensile rupture and the concrete compression failure. Once more, in an uncracked section where $d_f > d_s$ and $\varepsilon_f = \varepsilon_{fu}$, the condition of ($\varepsilon_s > \varepsilon_{sy}$) is true for a balanced-strengthened design of steel. By these presumptions the considering the limits of the strain, and with regards to compatibility and balance, the analytical balanced-strengthened of the FRP area is:

$$A_{fb} = \frac{0.85 f_c^{'} b \beta_1 d_f \left\{ \frac{\varepsilon_{cu}}{\varepsilon_{cu} + \varepsilon_{fu}} \right\} - A_s f_y}{f_{fu}} \tag{1}$$

If we consider the Eq. (1) as a theoretical limit of the FRP reinforcement, when $A_f > A_{fb}$, then failure is equal to the tensile rupture of the FRP. Also, when $A_f < A_{fb}$ the failure is the compression failure of the concrete. In fact, a negative or positive A_{fb} is valid, according to the existing amount of steel reinforcement (A_s). When a negative result id obtained from the Eq. (1), A_f is always larger than A_{fb} which indicates FRP failure concrete compression failure. Fig (2) shows the distribution of FRP failure, balanced-strengthened, and compression failure. In sections where FRP failure occurs, the following equilibrium is used to calculate the depth of compression block (a) as well as the nominal moment strength at ultimate M_n.

$$\mathrm{a} = \frac{A_f f_{fu} + A_s f_y}{0.85 f_c^{'} b} \text{ for } \mathrm{A}_f < A_{fb} \tag{2a}$$

$$M_n = A_f f_{fu} (d_f - \frac{a}{2}) + A_s f_y (d_s - \frac{a}{2}) \text{ for } \mathrm{A}_f < A_{fb} \tag{2b}$$

According to Fig (2), in sections where concrete crushing occurs, the steel stress level is not known initially, according to Fig (2). When steel and concrete strains are fixed at yield ε_{sy} and crushing ε_{cu}, respectively, and the steel area corresponding to yield A_{sy} is determined, comparing it with the area of steel present, this value can be determined. Using Fig (2), the procedure results the following equation:

$$A_{sy} = \frac{0.85 f_c^{'} b \beta_1 d_s (\frac{\varepsilon_{cu}}{\varepsilon_{cu} + \varepsilon_{sy}}) - A_f E_f \varepsilon_{sy} (\frac{d_f}{d_s})}{f_y} \tag{3}$$

Likewise, the steel stress is f_y when $A_s \leq A_{sy}$. However, in case of $A_s > A_{sy}$, the steel stress is less than f_y and have to be calculated by compatibility and equilibrium. By use of this method, in all samples controlled by concrete failure in this study the ultimate steel stress was equal to yield. While the steel stress is equal to yield, for the sections controlled by concrete failure, the compression block (a), FRP reinforcement stress (f_f), and nominal moment capacity (M_n) can be obtained from the following equations:

$$a = \frac{\sqrt{(A_f E_f \varepsilon_{cu} - A_s f_y)^2 + 4(0.85) f_c^{'} b \beta_1 A_f E_f \varepsilon_{sy} d_f} - (A_f E_f \varepsilon_{cu} - A_s f_y)}{(2)0.85 f_c^{'} b} \tag{4a}$$

$$f_f = E_f \varepsilon_{cu} \frac{d_f - \alpha / \beta_1}{\alpha / \beta_1} \leq f_{fu} \tag{4b}$$

$$M_u = A_f f_f (d_f - \frac{a}{2}) + A_s f_y (d_s - \frac{a}{2}) \tag{4c}$$

3. Artificial neural networks methodology

Artificial neural networks are not commonly employed for the purpose of estimating the capacity of civil engineering structures. However, their inherent capability to effectively identify and replicate patterns renders them an ideal tool for undertaking such a task [23]. In the context of FRP strengthening of RC beams, these models assume a highly specialized role since they possess the capability to address intricate issues that prove challenging to resolve by analytical methods [24]. This is particularly true in cases when there is a lack of fundamental physical or mathematical models to guide the resolution of these challenges. Neural-network modelling, a nonlinear regression model utilized in the life sciences, is grounded on the basic mechanisms of the human brain [25]. Figure 3 illustrates the representation of typical computational neurons. The computational neuron possesses analogous characteristics to biological neurons, including an input, a nerve cell, and an output. The primary step in the modelling of neural networks in the present study involved the collection of homogeneous experimental data through a comprehensive analysis of previous studies and identified and selected the variables that have a significant impact on the outcome. These variables were subsequently designated as input nodes in the modelling procedure. In a neural network architecture, a node situated on a distinct layer is responsible for receiving a collection of input values and generating a linear output by utilizing weights and biases [26]. Neurons exhibit binary activation states, determined by an activation function. The primary objective of the activation function is to derive non-linear output from a linearly generated value. The Sigmoid, Tanh, and Rectified Linear Unit (ReLU) functions are widely recognized as the three most prominent activation functions in the field [25]. In the domain of civil engineering, it has been observed that the Tanh function exhibits superior performance compared to alternative activation functions when employed as the output layer

activation function [27]. In order to enhance the predictability of the proposed prediction model, several neurons were interconnected to create an Artificial Neural Network (ANN).

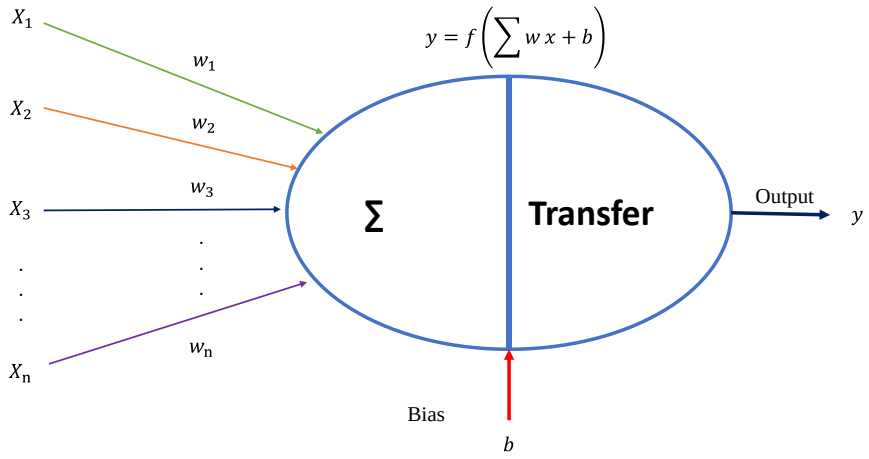

Fig. 3. Schematic of computational neurons [28].

This neural network consists of one or more hidden layers, an output layer, and a multilayer perceptron. The architecture of a multilayer perceptron is seen in Figure 5. The architecture of artificial neural network (ANN) models has a significant impact on their implementation [29]. While there exist alternative training processes, the backpropagation (BP) algorithm is generally known to produce satisfactory outcomes [30]. The Levenberg-Marquardt method is often employed as a post-release training algorithm [24]. Prior to the training phase, the acquired data, consisting of inputs and targets, undergoes normalization or scaling based on known relationships. This is achieved by reducing the disparity between the values of the variables under examination across different scales. The equation, denoted as Eq. (1), is employed to standardize relationships, wherein the values are confined within the range of 0.1 to 0.9, as observed in the relationships enumerated below:

$$I_S = \frac{(0.9-0.1)(I-I_{min})}{I_{max}-I_{min}} + 0.1 \tag{5}$$

The Levenberg-Marquardt method is utilized to randomly create three sets of input and target vectors, namely training, validation, and test sets. Various relative percentages are commonly considered, but, in order to optimize the distribution of the dataset, the training, validation, and testing subsets are typically allocated 70%, 15%, and 15% respectively [31]. The termination criterion for network training is determined by the mean square error, specifically by evaluating the squared difference between the network's outputs and the desired objectives. Lower mean squared error (MSE) values are associated with improved network performance. Regression values, which assess the degree of correlation between the outputs of a network and its targets, have become the prevailing criterion for selecting the appropriate stopping point for a network. Regression coefficients with a value of 1 indicate a substantial association, whereas regression coefficients with a value of 0 imply a chance occurrence. By considering these two parameters, one may effectively determine the optimal network [32]. The formation of the optimal network occurs through the selection of desirable networks and the careful consideration of the aforementioned criteria.

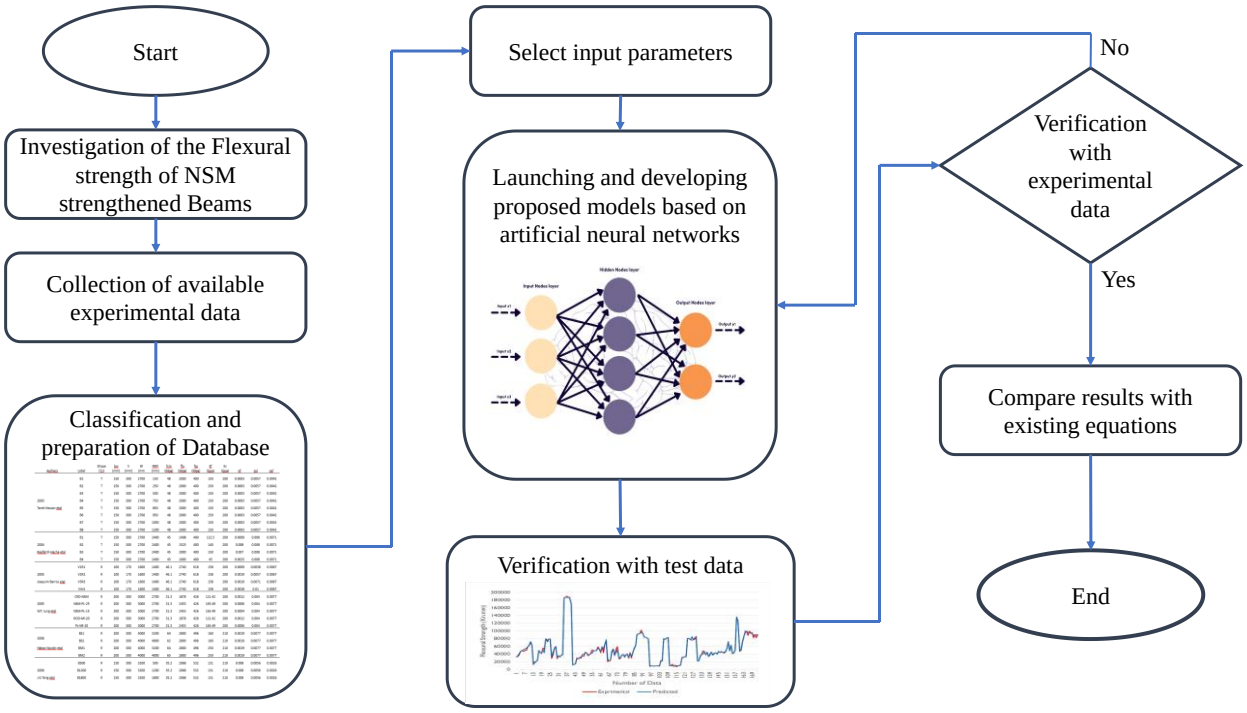
Start
Investigation of the Flexural strength of NSM strengthened Beams
Collection of available experimental data
Classification and preparation of Database
Select input parameters
Launching and developing proposed models based on artificial neural networks
Verification with test data
Verification with experimental data
No
Yes
Compare results with existing equations
End

Fig. 4. A present research program flow chart consists of the proposed model.

As previously mentioned, in this study a feed forward MLP neural network was employed, consisting of three layers: input, hidden, and output. The input layer represents the characteristic properties of the behavior of strengthened beams. Given the significant impact of numerous elements on the Flexural failure mode, it is imperative to meticulously pick input variables or signatures to achieve an optimal configuration of the Artificial Neural Network (ANN). This is due to the necessity of selecting the number of input parameters in accordance with the quantity of training data. In order to accurately describe the system, a multitude of parameters must be carefully selected. However, it has been established that an increased quantity of input neurons has a detrimental effect on the efficiency and accuracy of the training process in artificial neural networks (ANNs).

The activation functions of tan-sigmoid and linear are employed in their respective activation functions. Training trials were employed to find the optimal number of hidden layer nodes and determine the most suitable activation functions. The programming language MATLAB was utilized to develop, train, and deploy an Artificial Neural Network (ANN) employing the back-propagation technique and the Levenberg-Marquardt training algorithm. The artificial neural network (ANN) was trained iteratively with the objective of minimizing the performance function, namely the mean square error (MSE), between the network outputs and the associated goal values. In a general trend, it was observed that increasing the number of input-target pairings used during the training process resulted in a higher level of generalization capacity for the training artificial neural network (ANN) [33].

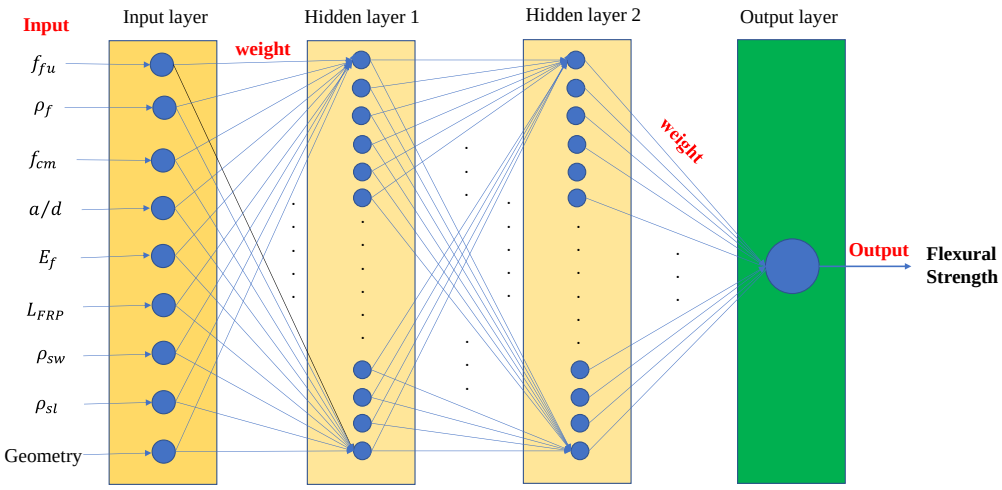

Fig. 5. ANN Model Architecture.

4. Database and models

In order to configure and train the ANN, 171 experimental tests collected from 39 NSM-FRP-flexural strengthened concrete beams experimental articles [2,13,38–47,14,48–57,16,58–65,20,21,34–37]. Table 1 shows the database sample. With regards to the beam geometric ratios, ratios of reinforcement, the characteristics of the materials and failure loads the chosen dataset show a high diversity. The database was categorized randomly into three sets: A training set that contained 70% beams, a validating set using 15% of the beams, and a test set with 15% total data. The input and output data were scaled between the interval [0.1, 0.9], in order to prohibit the slow learning rate of at the end points.

5. Prediction of the flexural capacity of NSM-FRP strengthened RC beams using ANNs

For the data set related to the beam flexural capacity presented here, just 1 output node was configured in the ANN. However, as previously mentioned among the large range of elements influencing the behavior of this strengthening approach, the correct selection of the input parameters is essential for a successful procedure. As a result, we divided the process of configuring and training the ANN into two steps. After a thorough analysis of the literature in the first phase, fifteen parameters were selected for the input: (a) beam geometry, which was either rectangular or T section, (b) NSM-FRP reinforcement ρ_f ratio, (c) f_{cm} (concrete average compressive strength) (d) a/d shear span/depth ratio, (e) distance between FRP bars edge to support L_d ,(f) elastic modulus of the FRP reinforcement w_1, (g) design yielding stress of the steel reinforcement f_{sy}, (h) FRP length L_{FRP}, (i) ratio of the steel shear reinforcement ρ_{sw}, (j) ratio of the steel longitudinal reinforcement ρ_{sl}, (k) height of the beam section h, (l) length of the beam L_B, (m) FRP ultimate strength f_{fu} (n) width of the beam cross section b_w (o) and elastic modulus of the steel reinforcement E_s.

Table 1
Flexural Database Sample.

Authors	Label	*Shape (T, R)*	b_w *(mm)*	h *(mm)*	L_B *(mm)*	L_{FRP} *(mm)*	f_{cm} *(MPa)*	f_{fu} *(MPa)*	f_{sy} *(MPa)*	E_f *(GPa)*	E_s *(GPa)*	ρ_f	ρ_{sl}	ρ_{sl}'
Hassan and Rizkalla 2003 [66]	B1	T	150	300	2700	150	48	2000	400	150	200	0.0003	0.0057	0.0042
	B2	T	150	300	2700	250	48	2000	400	150	200	0.0003	0.0057	0.0042
	B3	T	150	300	2700	500	48	2000	400	150	200	0.0003	0.0057	0.0042
	B4	T	150	300	2700	750	48	2000	400	150	200	0.0003	0.0057	0.0042
	B5	T	150	300	2700	850	48	2000	400	150	200	0.0003	0.0057	0.0042
	B6	T	150	300	2700	950	48	2000	400	150	200	0.0003	0.0057	0.0042
	B7	T	150	300	2700	1050	48	2000	400	150	200	0.0003	0.0057	0.0042
	B8	T	150	300	2700	1200	48	2000	400	150	200	0.0003	0.0057	0.0042
El-Hacha et al. 2005 [6]	B1	T	150	300	2700	2400	45	1408	400	122.5	200	0.0009	0.008	0.0071
	B2	T	150	300	2700	2400	45	1525	400	140	200	0.008	0.008	0.0071
	B3	T	150	300	2700	2400	45	2000	400	150	200	0.007	0.008	0.0071
	B4	T	150	300	2700	2400	45	1000	400	45	200	0.0025	0.008	0.0071
Barros et al. 2004 [19]	V1R1	R	100	170	1600	1400	46.1	2740	618	158	200	0.0009	0.0038	0.0067
	V2R2	R	100	170	1600	1400	46.1	2740	618	158	200	0.0019	0.0057	0.0067
	V3R3	R	100	170	1600	1400	46.1	2740	618	158	200	0.0019	0.0071	0.0067
	V4r4	R	100	170	1600	1400	46.1	2740	618	158	200	0.0028	0.01	0.0067
Jung et al. 2005 [67]	CRD-NSM	R	200	300	3000	2700	31.3	1878	426	121.42	200	0.0012	0.004	0.0077
	NSM-PL-25	R	200	300	3000	2700	31.3	2453	426	165.49	200	0.0006	0.004	0.0077
	NSM-PL-15	R	200	300	3000	2700	31.3	2453	426	165.49	200	0.0004	0.004	0.0077
	ROD-Ml-20	R	200	300	3000	2700	31.3	1878	426	121.42	200	0.0012	0.004	0.0077
	PL-Ml-20	R	200	300	3000	2700	31.3	2453	426	165.49	200	0.0006	0.004	0.0077
Nordin and Täljsten 2006 [12]	BS1	R	200	300	4000	3200	64	2800	496	160	210	0.0019	0.0077	0.0077
	BS2	R	200	300	4000	4000	62	2800	496	160	210	0.0019	0.0077	0.0077
	BM1	R	200	300	4000	3200	64	2800	496	250	210	0.0019	0.0077	0.0077
	BM2	R	200	300	4000	4000	65	2800	496	250	210	0.0019	0.0077	0.0077
Teng et al. 2006 [9]	B500	R	150	300	3200	500	35.2	2068	532	131	210	0.008	0.0056	0.0026
	B1200	R	150	300	3200	1200	35.2	2068	532	131	210	0.008	0.0056	0.0026
	B1800	R	150	300	3200	1800	35.2	2068	532	131	210	0.008	0.0056	0.0026
	B2900	R	150	300	3200	2900	35.2	2068	532	131	210	0.008	0.0056	0.0026
Tang et al. 2006 [17]	SPA40-G5-A	R	180	250	1500	1500	21	512	398	64	252	0.0106	0.0106	0.0014
	SPA20-G5-A	R	180	250	1500	1500	37	512	398	64	252	0.0106	0.0106	0.0014
	SPA20-G3-A	R	180	250	1500	1500	37	650	398	64	252	0.0037	0.0106	0.0014
	SNC-G5-A	R	180	250	1500	1500	58	512	398	64	252	0.0106	0.0106	0.0014
	SNC-G5-B	R	180	250	1500	1500	58	512	398	64	252	0.0106	0.0106	0.0014
Al-Mahmoud et al. 2009 [63]	B1	T	150	400	4000	4000	49.5	2068	558	131	210	0.0005	0.0033	0.0031
	B2	T	150	400	4000	4000	52.8	2068	558	131	210	0.0005	0.0033	0.0031
	C1	T	150	400	4000	4000	52.7	1970	558	147	210	0.0004	0.0033	0.0031
	C2	T	150	400	4000	4000	50.1	1970	558	147	210	0.0004	0.0033	0.0031
	D1	T	150	400	4000	4000	50.1	690	558	40.8	210	0.0013	0.0033	0.0031
	D2	T	150	400	4000	4000	35.2	690	558	40.8	210	0.0013	0.0033	0.0031
Barros and Kotynia 2008 [68]	S1	R	120	170	1000	1000	44.2	2740	788	158.8	200	0.0009	0.0025	0.0025
	S2	R	120	170	1000	1000	44.2	2740	627	158.8	200	0.0017	0.0043	0.0025
	S3	R	120	170	1000	1000	44.2	2740	627	158.8	200	0.0026	0.0064	0.0025

Through randomly choosing the training sample and applying the sensitivity analysis (Milne index) to every model that satisfied the primary criteria, A preliminary filter was applied to the input parameters. Using operations between the weight matrices produced in two adjacent layers of the ANN, the Milne index may determine the relative importance of all input variables in relation to the output variable [29]. The strategy can be helpful in situations where the index differs significantly amongst the trained networks. On the other hand, if an input parameter's index remains low across a large number of networks, it suggests that the parameter is irrelevant and should be removed.

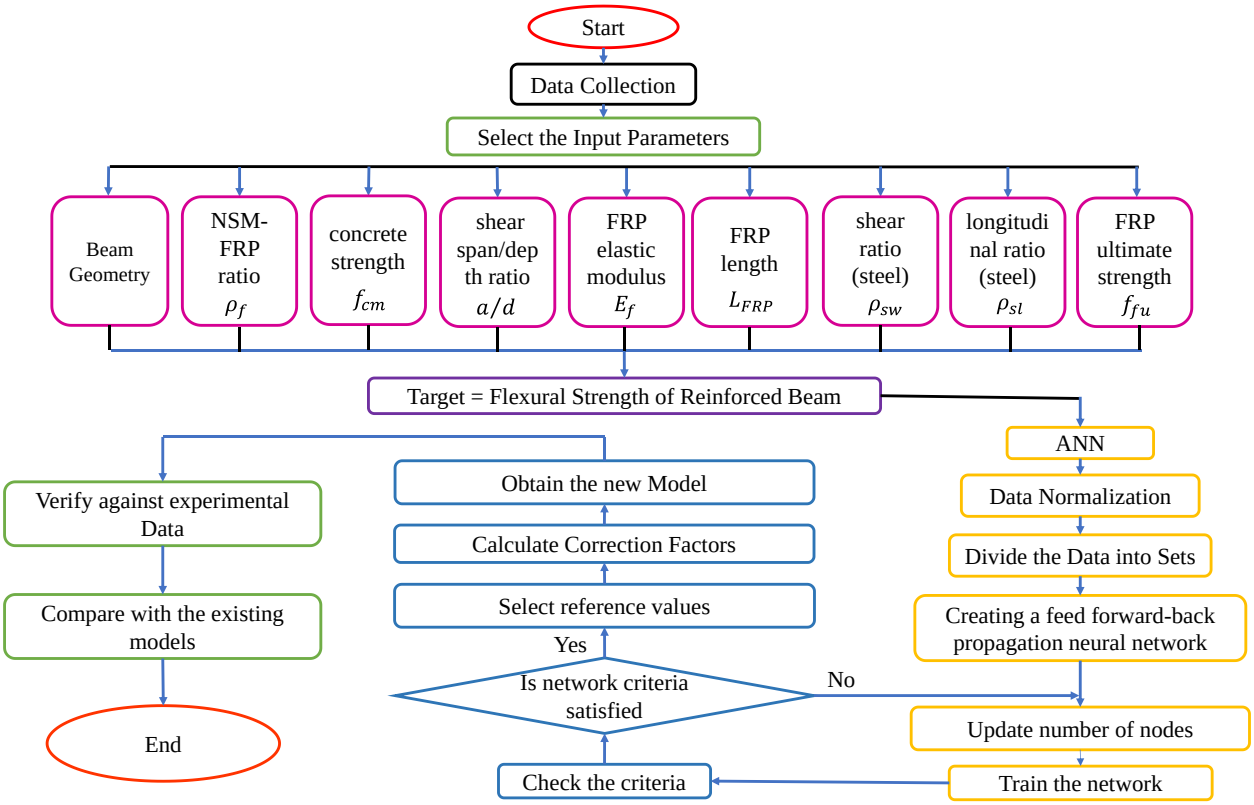

Fig. 6. Specific details of the proposed ANN Model.

The beam length and the steel reinforcement's E_s elastic modulus was removed in the first phase. The following condition involved a parametric analysis to assess how well each trained network can depict the impact of each specific input parameter on the beam capacity. These investigations were carried out by altering one input parameter while leaving the other unchanged. The effectiveness of different ANNs in mimicking the physical behavior of the flexural strengthening of an RC beam was confirmed by parameter analysis. Additionally, for every set of input parameter, there were between 8 and 20 hidden nodes, and training was carried out for every possible configuration. a/d shear span/depth ratio and ratio of the steel shear reinforcement ρ_{sw} were found to be less effective in ANN at the second phase. The final 10 variables were used as input variables. For each network, the mean square error between its output after training and the associated target values in the training and validation sets is initially estimated. The MSE value was smaller, hence the evaluated network received a higher point. The ANNs whose predictions agreed with the results of the experimental testing would produce

qualitative proof of the ANN's capacity to imitate the physical phenomenon. In order to compare the experimental results and assess each network's quality, potential anomalies relating to the network's behavior for a given parameter were identified. This was followed by a comparison of the predictions made by each network. This parametric evaluation led to the awarding of points to each network and parameter. The following were the network parameters used in this study: A hidden layer with 16 hidden neurons has one output parameter and ten input parameters.as displayed in Figure 7.

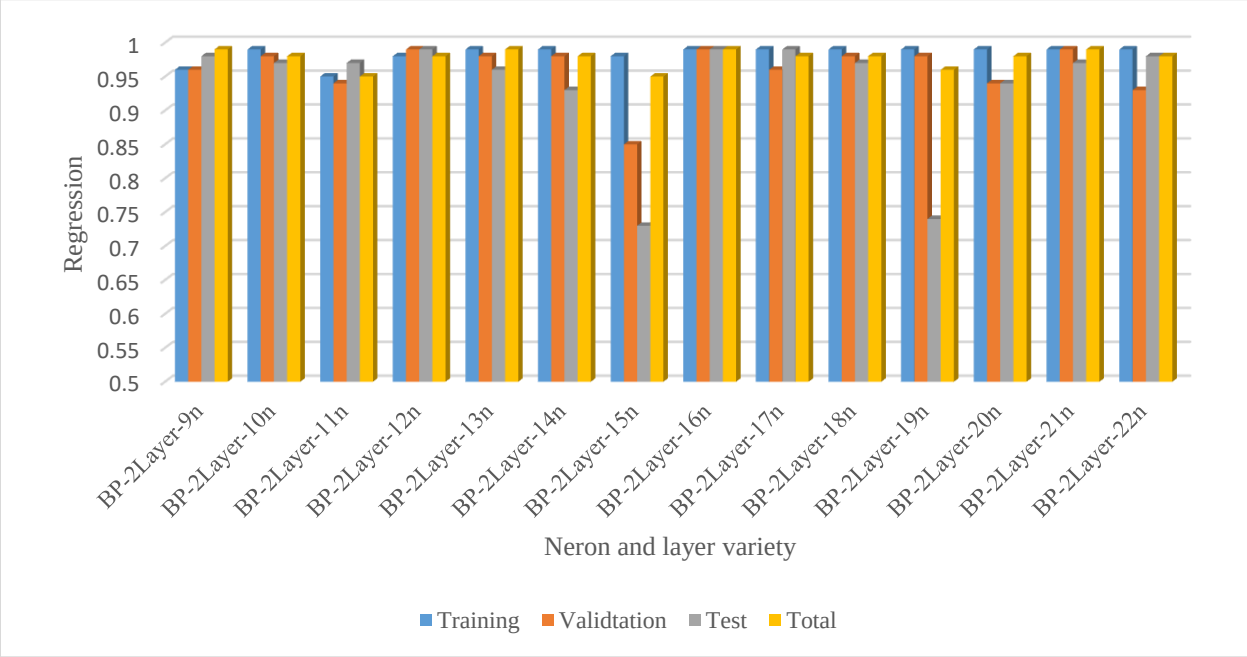

Fig. 7. Best fitted models based on number of neurons and hidden layers.

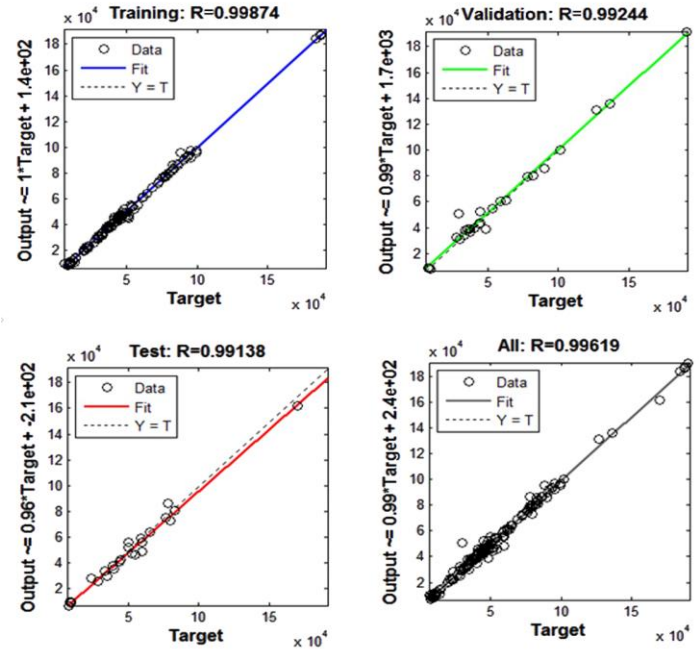

Fig. 8. Final ANN Regression.

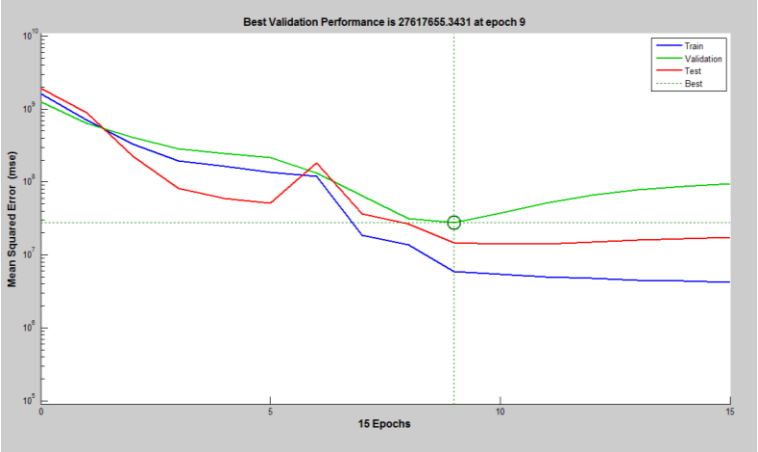

Fig. 9. Flexural ANN with 1 hidden layer and 16 hidden neurons.

The proposed ANN model could predict the flexural strength of NSM strengthened beams with mean absolute error of just 5% in comparison to the experimental results. Figures 10 through 12 illustrate how ANNs outperform conventional models in terms of capacity prediction. However, from the standpoint of engineering design, it may be argued that using straightforward design equations is a more useful method for determining the strength of NSM-FRP Flexure strengthened beams. The current study's proposal of design equations to determine the flexure capacity of RC beams NSM-FRP strengthened in flexure is one of its objectives. In accordance with the observed behavior of the analyses performed using neural networks, we suggest an optimization strategy to generate simple and accurate flexure design equations for NSM-FRP flexure reinforced RC beams. The optimization strategy is created in GMDH [24] due to the fact that GMDH algorithms are specifically suitable for handling multi objective issues.

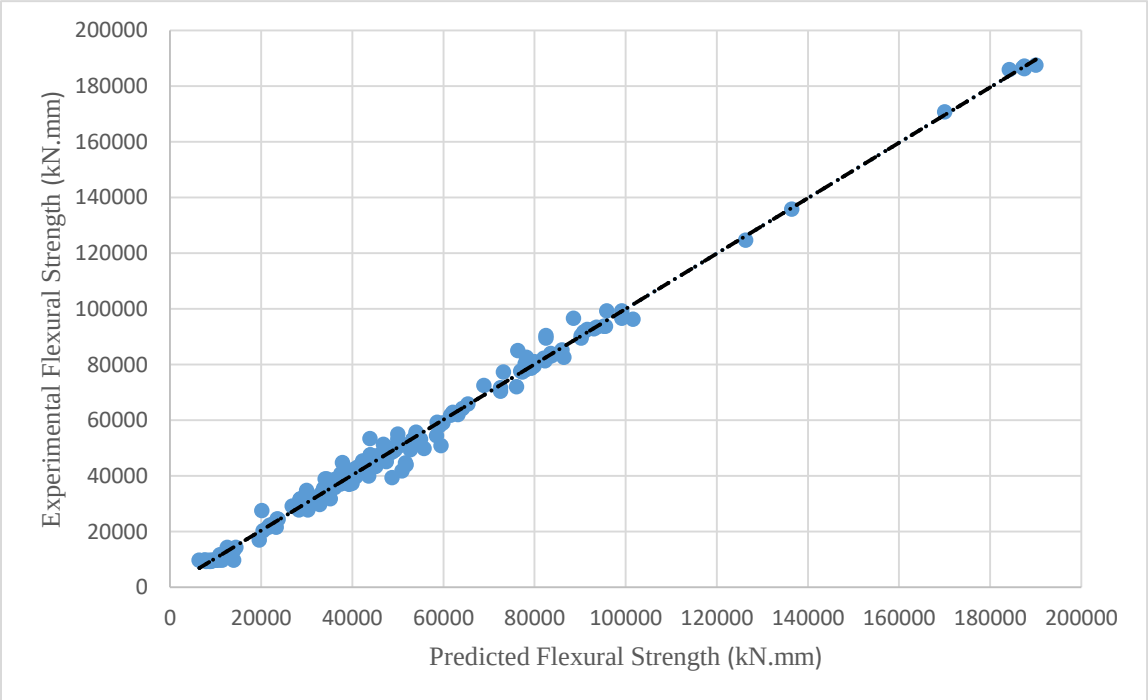

Fig. 10. ANN Predicted Flexural Strength comparison with Experimental.

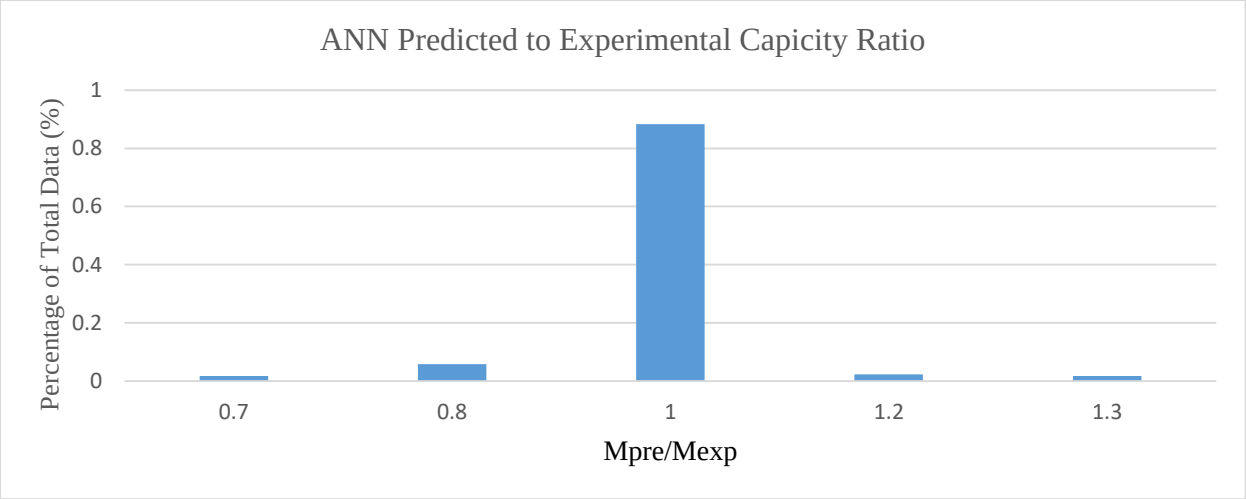

Fig. 11. ANN Predicted to Experimental Capacity Ratio.

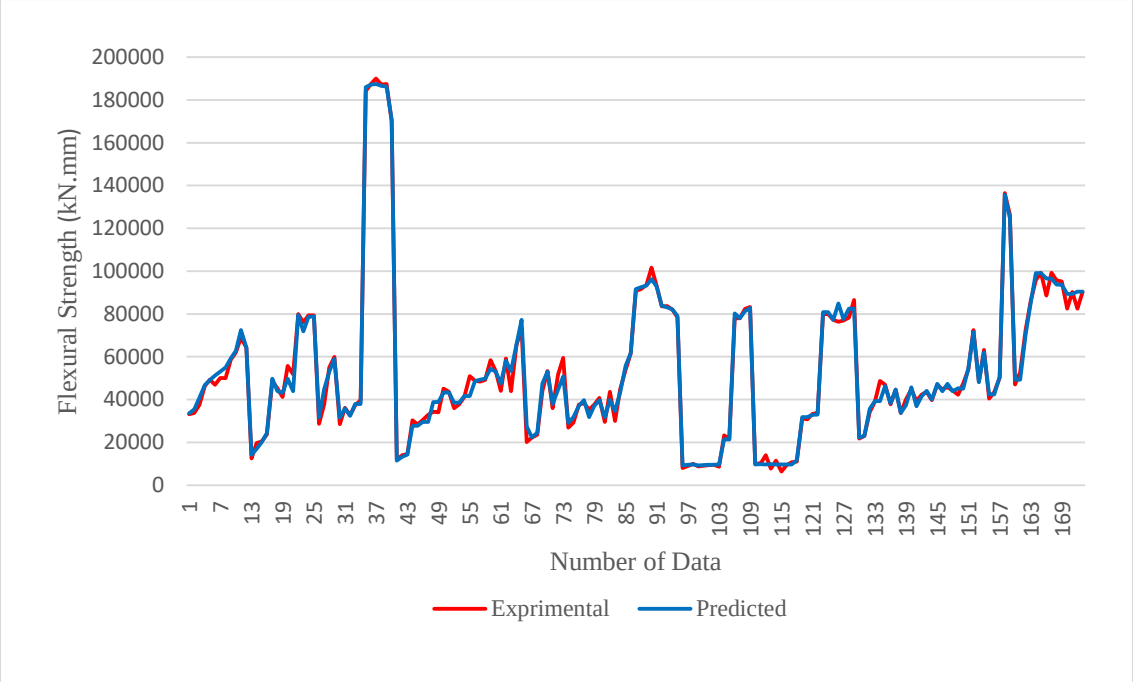

Fig. 12. Experimental to ANN predicted Flexural Strength point to point comparison

6. Proposing equation for prediction of flexural strength of reinforced sections using GMDH algorithm

Broadly speaking, the field of neural networks can be approached from two primary approaches when it comes to their introduction and recognition. From one perspective, neural network can be considered as autonomous entities characterized by diverse network structures and a strong capacity for identification and modeling. From an alternative standpoint, neural networks serve as a scientific instrument for the application and understanding of intricate mathematical methods. In contradistinction to the initial perspective, this theoretical framework incorporates the utilization of networks through algorithmic processes. In essence, neural networks can be

conceptualized as graphical representations of intricate mathematical procedures. When considering the group method of data handling (GMDH) neural networks, it is important to examine the neural networks from a second perspective. This construction has a substantial influence on the implementation of software and the understanding of GMDH neural networks. Hence, the utilization of self-organizing neural networks within the GMDH algorithm has resulted in the effective exploration of many domains by these networks, including technological, engineering, scientific, and economic fields in recent times. Consequently, this particular viewpoint is employed to present a mathematical framework for forecasting the flexural strength of a beam that has been reinforced using the NSM technique. This part pertains to the use of dimensional analysis to network input parameters and the utilization of neural network findings in conjunction with a simplified mathematical model. The objective is to effectively utilize six variables with energy and displacement dimensions as inputs for the GMDH network. The variables chosen for analysis include L_d , L_f, f_{ssh}, f_{fssh} , f_{csh}, , $\frac{E_f}{E_s}$. These variables are derived from the parameters of a neural network discussed in the previous section, and they represent the desired dimensions of the system. It is important to note that these variables do not necessarily determine the proportion of each section's flexural capacity. In this section, we will provide a description of the variables specified and present the proposed model in the following manner:

$$M_r = f_{ssh}\left(9.2f_{csh} - 42.2f_{ssh} - 350.5L_f + 5399\frac{E_f}{E_s} + 75f_{fsh}\right) + f_{fsh}\left(1363\frac{E_f}{E_s} - 4950\right) - \frac{E_f}{E_s}\left(14860.8L_f + 247606.6\frac{E_f}{E_s} + 9055.8L_d - 27.44\right) + L_f(569.25L_d + 27772) - 159996 \tag{6a}$$

The variables are described as follows:

$$f_{ssh} = \rho_{sl} \times b \times H \times f_y \tag{6b}$$

$$f_{fsh} = \rho_f \times b \times H \times f_{fu} \tag{6c}$$

$$f_{csh} = f_c \times b \times H \tag{6d}$$

L_f: FRP length

L_d=: FRP edge distance from support

f_{csh} = Index representing concrete share

f_{fsh} = Index representing FRP share

f_{ssh} = Index representing steel rebars share

The equation presented above demonstrates that each input parameter follows an algebraic relationship with constant coefficients and a beginning value, resulting in the output of the

problem, which is the flexural strength of reinforced sections using the Near-Surface Mounted (NSM) approach. The practice of conducting dimensional analysis on input parameters serves the purpose of simplifying the mathematical model, rather than making any assertions about the network output or the flexural strength of the section being within the same dimension. Figure 13 displays the ratio between the flexural capacity determined by the proposed equation and the experimental results. The equation under consideration is assessed with precision, and the laboratory values obtained are compared in Figures 14 and 15.

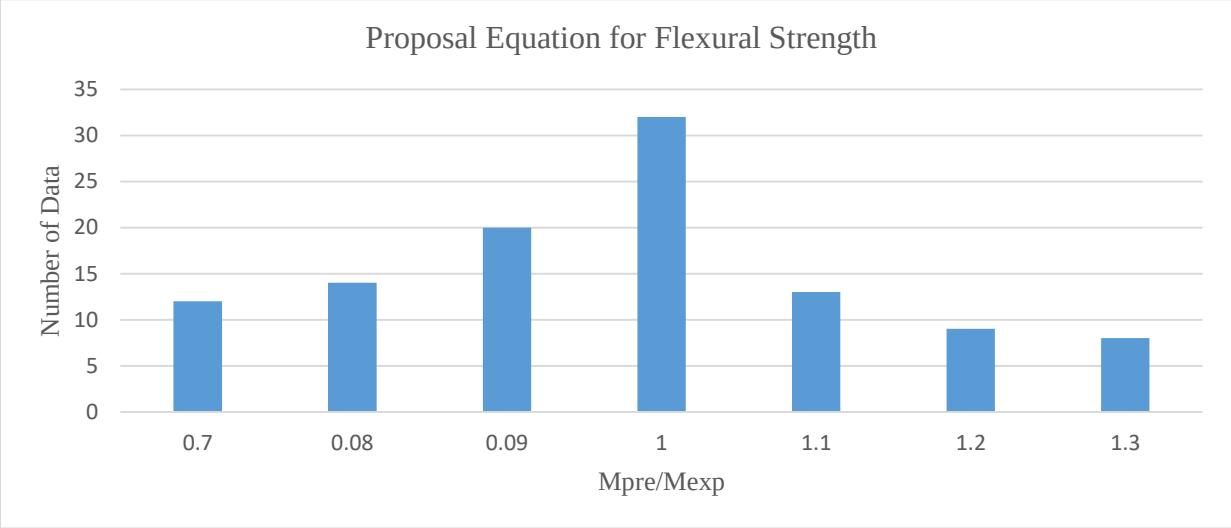

Fig. 13. Ratio of the proposed flexural capacity through the suggested equation to the laboratory flexural capacity.

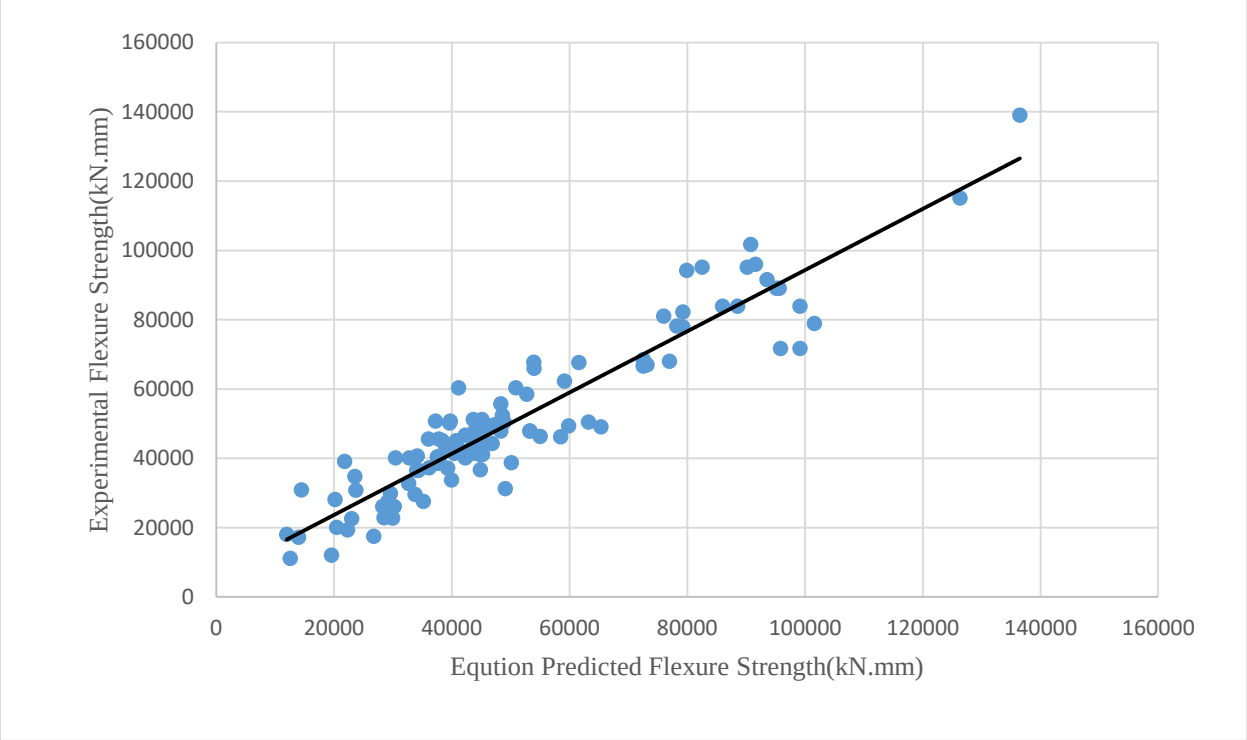

Fig. 14. Comparison of predictive data of the proposed equation and laboratory results.

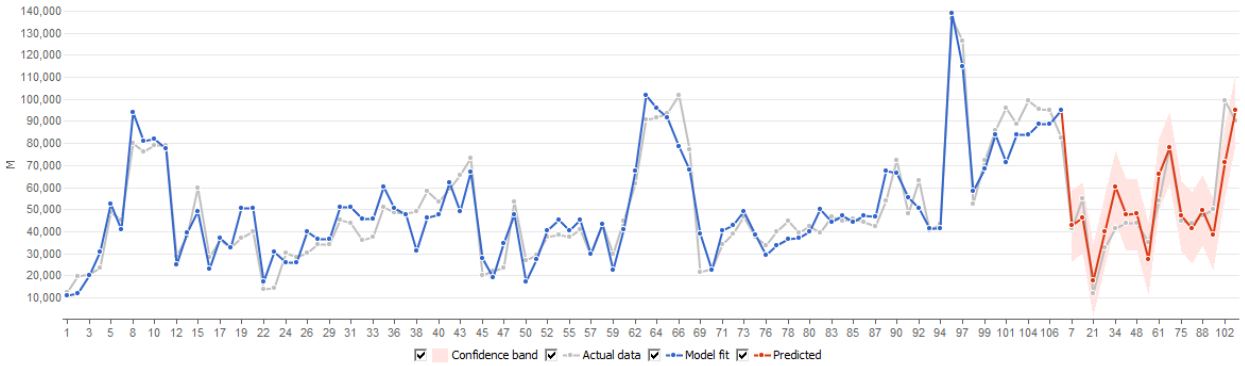

Fig. 15. Point-by-point comparison of laboratory and proposed flexural strengths by equation in training mode.

7. Comparison of the proposed equation with ACI 440.2R and FIB guideline

As indicated in the introductory section, there is currently no rule that provides a particular equation for the flexural capacity of reinforced beams using the Near Surface Mounted (NSM) approach. Hence, a comparison is made between the equation presented by ACI 440.2R [1], which is utilized for the estimate of flexural capacity of reinforced beams by the external bonded (EB) method, and the recommended equation. The equation for determining the flexural capacity of a reinforced section using the Equivalent Bending (EB) method as specified in the ACI440.2R regulation is derived by accounting for the contribution of each section of the element and incorporating the safety factor $\boldsymbol{\gamma_f}$ in the calculation of the flexural strength of the section's Fiber Reinforced Polymer (FRP) component. Based on empirical observations, it is postulated that the fiber-reinforced polymer (FRP) profile in the specified segment attains its ultimate strength. In the context of the regulation pertaining to external bonded reinforcement, it has been observed that the equation proposed for determining the share of FRP flexural capacity in relation to the total capacity does not incorporate the safety factor $\boldsymbol{\gamma_f}$. The equation governing the regulation and its associated variables are delineated as follows:

$$M_{Rd} = A_{sl} \times f_{syd}(d_s - 0.4x) + \gamma_f A_f f_{fe}(h - 0.4x) \tag{7a}$$

$$f_{fe} = E_f * \varepsilon_{fu} \tag{7b}$$

$$\gamma_f = 0.85 \tag{7c}$$

The comparison between the flexural capacity of the section, as determined by the ACI440.2R regulation, and the flexural capacity estimated by the proposed model, is presented in Figure 17 alongside the test data. Based on the visual representation provided, it can be inferred that the occurrence of FRP rupture resulted in a notable disparity between the flexural capacity as estimated by regulatory guidelines and the outcomes obtained from laboratory experimentation. This assumption highlights a significant discrepancy in the ability to accurately predict the

flexural capacity of a section reinforced by the Near-Surface Mounted (NSM) method compared to the Externally Bonded (EB) technique. This discrepancy arises from the larger cross-sectional area of Fiber Reinforced Polymer (FRP) profiles used in the NSM method, as opposed to the FRP sheets employed in the EB technique. It is important to note that this assessment is subjective and requires verification to establish its validity.

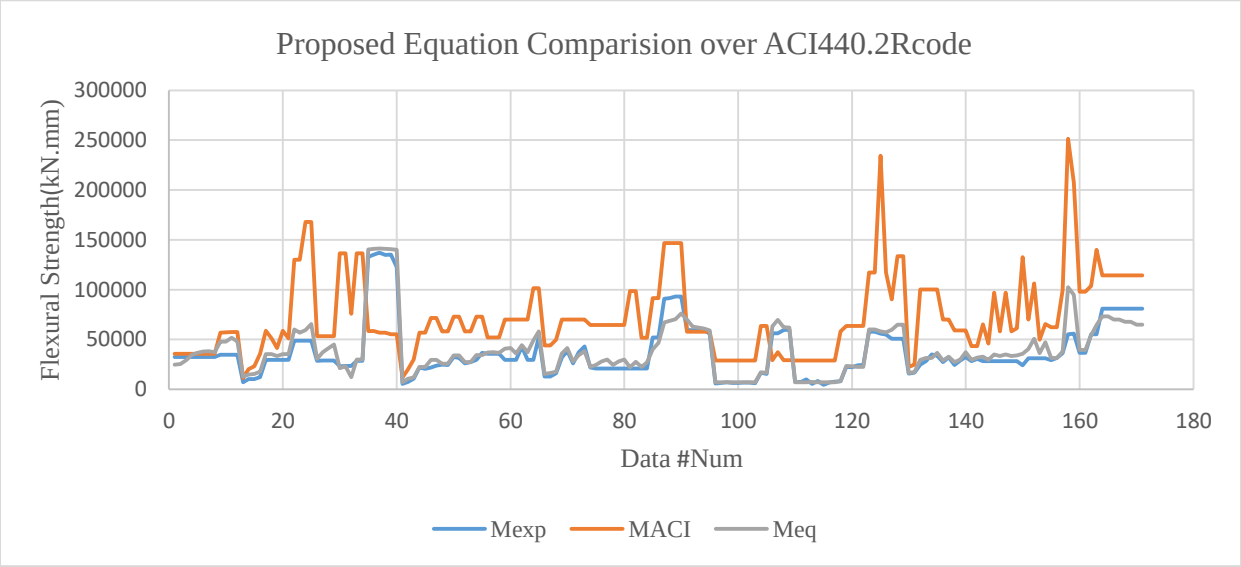

Fig. 16. Comparison of the capacity estimated by the equation of ACI440.2R regulation and laboratory results.

In the updated edition of the ACI440.2R regulation [69], the aforementioned equation has been substituted with the utilization of a traditional analytical equation that is based on fundamental assumptions. The accuracy of this equation is evaluated in accordance with the calculations performed. In these estimations, the initial assumption considers only two primary modes of failure for the sample, namely the crushing of compressive concrete and the rupture of the FRP profile. The accuracy and error of the dimensions of the neural axis site are taken into consideration. Furthermore, the estimation of strain in fiber-reinforced polymer (FRP) concrete and profile is conducted under the assumption that the strain exhibits linearity across the section. The dominance of FRP profile rupture assumption is contingent upon the strain obtained being greater than the maximum strain exhibited by the FRP material. Furthermore, the maximum tensile strength of the Fiber Reinforced Polymer (FRP) profile is considered to be the utmost measure of energy and strain. Subsequently, the strain and energy of metal rebar are computed by employing the principle of strain adaptation within the section. The determination of the neutral axis location is achieved by employing mathematical formulae, which are afterwards utilized to evaluate its position. This computed value is then compared to the initial assumption made, and any necessary adjustments are made accordingly. The method presents challenges in both the initial determination and subsequent verification of the primary estimate for the neutral axis, which can impact the overall accuracy of the final selection. Furthermore, it should be noted that

the hypotheses put forth in this study do not include the assumption of FRP profile rupture in the section reinforced by the NSM method, nor do they account for the evaluation of adhesion resistance between sample surfaces and failure modes. It is worth mentioning that less than 30% of the laboratory data utilized in this research resulted in FRP profile rupture. Hence, it is recommended that key assumptions be carefully chosen in order to strengthen the parts supported by the NSM technique. The comparison between the laboratory results and the flexural strength of the sections reinforced by the NSM method, as per the ACI440.2R regulation and the suggested equation, is depicted in Figure 13. The figure (13) demonstrates that the ACI440.2R rule possesses the capability to forecast the flexural capacity of a section when compared to laboratory results, exhibiting a mean absolute error of 32% in terms of insurance. It is important to acknowledge that the extent of this disparity is heavily contingent upon the precision with which the primary condition is chosen and the amounts of corrections made to account for any inaccuracies inherent in the equations. This study aims to develop models that accurately represent the examples of theory addressed in the ACI440.2R regulation, with a focus on selecting the primary assumption. Moreover, the suggested equation exhibits a satisfactory convergence to laboratory results, as evidenced by its mean absolute error rating of 16%. The evaluation of the ratio between the projected capacity determined by these approaches and the test results is conducted in the subsequent section in order to ascertain the equation's safety. Despite its improved potential for predictive accuracy, the suggested equation for estimating flexural capacity occasionally overestimated the capacity in 5% of situations, with a maximum inaccuracy of 29% compared to laboratory capacity. Additional findings are presented in figures 19 and 20.

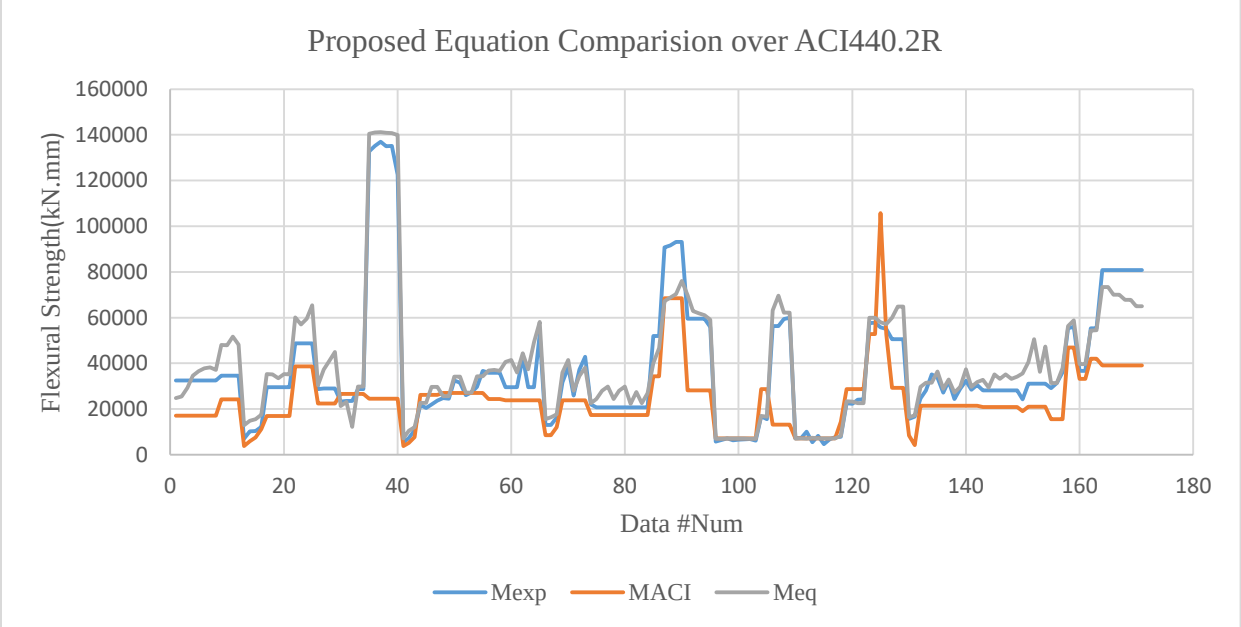

Fig. 17. Comparison of capacity estimated by ACI440.2R regulation and laboratory results.

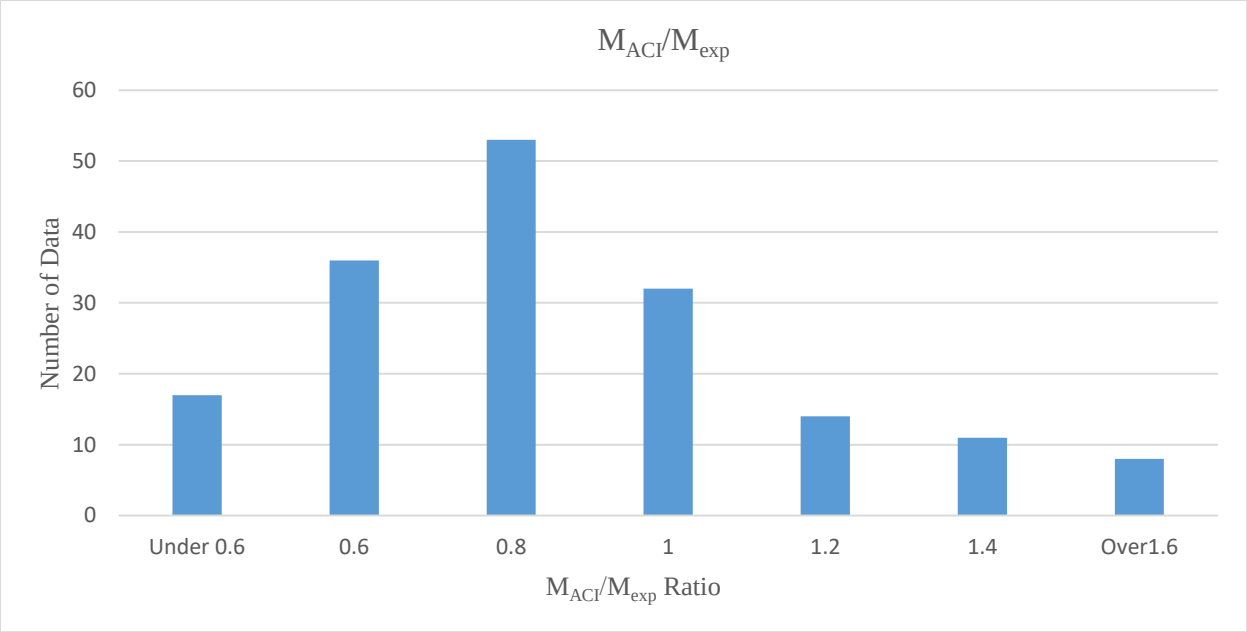

Fig. 18. Ratio of flexural capacity of ACI440.2R equation to laboratory results.

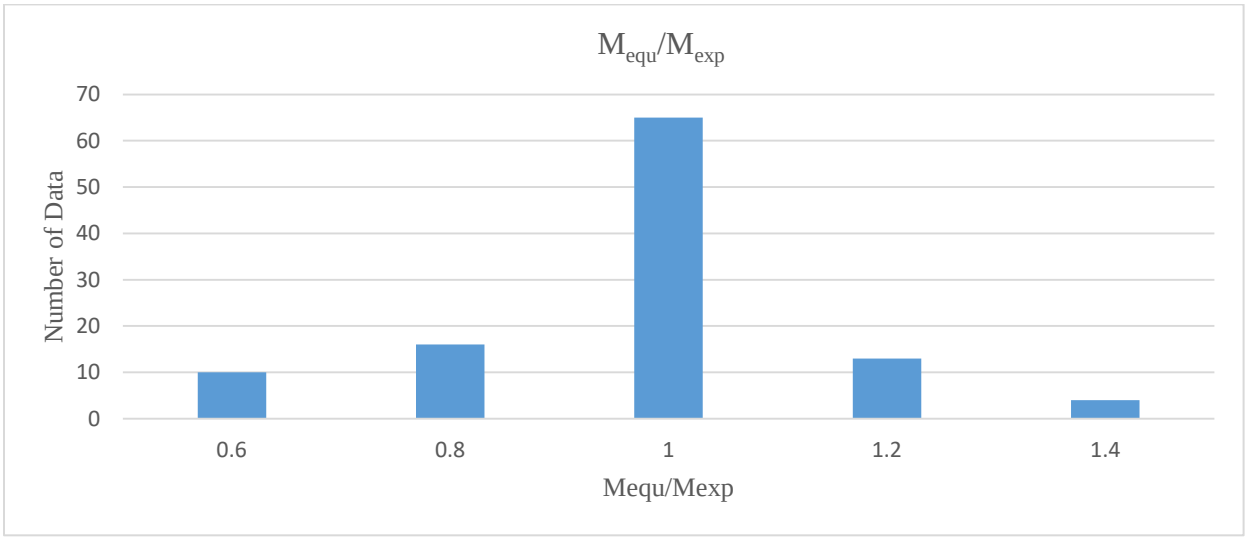

Fig. 19. Ratio of flexural capacity predicted by the proposed equation to the laboratory flexural capacity.

8. Conclusions

The current study involved the collection of a database containing laboratory findings pertaining to the capacity of concrete beams reinforced with the Near-Surface Mounted Fiber Reinforced Polymer (NSM-FRP) technology. The subsequent phase involved the evaluation of the influential factors that contribute to the determination of the flexural resistance of reinforced beams. In order to accomplish this, a comprehensive analysis was conducted on a total of 32 scholarly articles that specifically address the topic of flexural failure in reinforced beams. These articles encompass the entirety of published research on the subject up until the present time. The compiled database comprised the study outcomes of diverse studies conducted at numerous

research institutions, each of which took into account these factors during their experimental investigations. When selecting the input parameters for models, it is crucial to prioritize the use of fewer inputs in order to enhance accuracy, particularly when employing the GMDH neural network in modeling. The GMDH modeling approach was utilized to build a flexural capacity model consisting of 10 effective parameters. The evaluation and comparison of the modeling output results were conducted in accordance with the ACI 440.2 R requirements. Based on this study, the following conclusions were drawn:

- The elements that significantly affect the bending capacity of the cross-section were broadly categorized, and a sensitivity analysis was conducted to identify the top 10 parameters with the greatest impact.
- The neural network demonstrates a predictive capability in determining the flexural capacity of the reinforced cross-section when utilizing the near-surface mounted (NSM) technique. This prediction is achieved with an average absolute error of 5% and an overall regression value of 0.99.
- The equation derived from the GMDH method demonstrated a satisfactory correlation between the reinforced beam and its flexural capacity, with an average absolute error of 16% and a predictive percentage that was deemed acceptable. The correlation in the ACI 440.2R (2002) guidelines relating to the estimated Flexural resistance of EB method lacks the proper generalizability for the findings of the current research due to the FRP rupture hypothesis.
- The ACI 440.2R standards, specifically the analytical-interpretive technique, provide adequate generalizability in relation to the flexural capacity in the EB method. The current research findings indicate an average absolute inaccuracy of 31%.
- The majority of the projected capacities, as per the ACI 440.2R recommendations, were found to be within the acceptable safety range. However, it is important to note that the accuracy of these values heavily relies on the initial assumptions made, and making appropriate corrections to these assumptions might significantly impact the results.
- The proposed equation for estimating flexural capacity, despite its increased potential for predictive accuracy, resulted in capacity estimates that exceeded the laboratory capacity in 5% of cases, with a maximum inaccuracy of 29%.

Future research field

In future works, the bonding behavior on various planes will be regarded as the fundamental characteristic. Prior to making capacity predictions, the bonding index will be established and computed for each sample.

Funding

This research received no external funding.

Conflicts of interest

The authors declare no conflict of interest.

Authors contribution statement

A.R, H.N, M.K: Conceptualization; A.R, P.F: Data curation; A.R, H.N, M.K: Formal analysis; A.R, P.F: Investigation; A.R, H.N, M.K: Methodology; H.N, M.K: Project administration; FA: Resources; A.R: Software; H.N, M.K: Supervision; H.N, M.K: Validation; A.R: Visualization; A.R, H.N, M.K: Roles/Writing – original draft; A.R, H.N, M.K, P.F: Writing – review & editing.

References

[1] 440.2R-17: Guide for the Design and Construction of Externally Bonded FRP Systems for Strengthening Concrete Structures. 2017. https://doi.org/10.14359/51700867.

[2] Effiong JU, Ede AN. Experimental Investigation on the Strengthening of Reinforced Concrete Beams Using Externally Bonded and Near-Surface Mounted Natural Fibre Reinforced Polymer Composites—A Review. Materials (Basel) 2022;15:5848. https://doi.org/10.3390/ma15175848.

[3] Bilotta A, Ceroni F, Di Ludovico M, Nigro E, Pecce M, Manfredi G. Bond Efficiency of EBR and NSM FRP Systems for Strengthening Concrete Members. J Compos Constr 2011;15:757–72. https://doi.org/10.1061/(ASCE)CC.1943-5614.0000204.

[4] Lorenzis L De, Nanni A, Tegola A La. Strengthening of Reinforced Concrete Structures with Near Surface Mounted FRP Rods. Int. Meet. Compos. Mater., 2000, p. 1–8.

[5] De Lorenzis L, Nanni A. Bond between near-surface mounted fiber-reinforced polymer rods and concrete in structural strengthening. ACI Struct J 2002;99:123–32. https://doi.org/10.14359/11534.

[6] El-Hacha R, Rizkalla SH, Kotynia R. Modelling of Reinforced Concrete Flexural Members Strengthened with Near-Surface Mounted FRP Reinforcement. SP-230 7th Int. Symp. Fiber-Reinforced Polym. Reinf. Concr. Struct., vol. SP-230, American Concrete Institute; 2005, p. 1681–700. https://doi.org/10.14359/14916.

[7] Taleb Obaidat Y, Barham WS, Aljarah AH. New anchorage technique for NSM-CFRP flexural strengthened RC beam using steel clamped end plate. Constr Build Mater 2020;263:120246. https://doi.org/10.1016/j.conbuildmat.2020.120246.

[8] Jalali M, Sharbatdar MK, Chen J-F, Jandaghi Alaee F. Shear strengthening of RC beams using innovative manually made NSM FRP bars. Constr Build Mater 2012;36:990–1000. https://doi.org/10.1016/j.conbuildmat.2012.06.068.

[9] Teng JG, De Lorenzis L, Wang B, Li R, Wong TN, Lam L. Debonding Failures of RC Beams Strengthened with Near Surface Mounted CFRP Strips. J Compos Constr 2006;10:92–105. https://doi.org/10.1061/(ASCE)1090-0268(2006)10:2(92).

[10] Sharaky IA, Torres L, Comas J, Barris C. Flexural response of reinforced concrete (RC) beams strengthened with near surface mounted (NSM) fibre reinforced polymer (FRP) bars. Compos Struct 2014;109:8–22. https://doi.org/10.1016/j.compstruct.2013.10.051.

[11] Hassan TK, Rizkalla SH. Bond Mechanism of Near-Surface-Mounted Fiber-Reinforced Polymer Bars for Flexural Strengthening of Concrete Structures. ACI Struct J 2004;101:830–9. https://doi.org/10.14359/13458.

[12] Nordin H, Täljsten B. Concrete Beams Strengthened with Prestressed Near Surface Mounted CFRP. J Compos Constr 2006;10:60–8. https://doi.org/10.1061/(ASCE)1090-0268(2006)10:1(60).

[13] Kara IF, Ashour AF, Köroğlu MA. Flexural performance of reinforced concrete beams strengthened with prestressed near-surface-mounted FRP reinforcements. Compos Part B Eng 2016;91:371–83. https://doi.org/10.1016/j.compositesb.2016.01.023.

[14] Seo S, Choi K, Kwon Y, Lee K. Flexural Strength of RC Beam Strengthened by Partially De-bonded Near Surface-Mounted FRP Strip. Int J Concr Struct Mater 2016;10:149–61. https://doi.org/10.1007/s40069-016-0133-z.

[15] Wu G, Dong Z, Wu Z, Zhang L. Performance and Parametric Analysis of Flexural Strengthening for RC Beams with NSM-CFRP Bars. J Compos Constr 2014;18:1–10. https://doi.org/10.1061/(ASCE)CC.1943-5614.0000451.

[16] Costa IG, Barros JAO. Flexural and shear strengthening of RC beams with composite materials – The influence of cutting steel stirrups to install CFRP strips. Cem Concr Compos 2010;32:544–53. https://doi.org/10.1016/j.cemconcomp.2010.03.003.

[17] Tang WC, Balendran RV, Nadeem A, Leung HY. Flexural strengthening of reinforced lightweight polystyrene aggregate concrete beams with near-surface mounted GFRP bars. Build Environ 2006;41:1381–93. https://doi.org/10.1016/j.buildenv.2005.05.029.

[18] Boukhezar M, Samai ML, Mesbah HA, Houari H. Flexural behaviour of reinforced low-strength concrete beams strengthened with CFRP plates. Struct Eng Mech 2013;47:819–38. https://doi.org/10.12989/sem.2013.47.6.819.

[19] Barros J, Sena-cruz J, Dias S, Ferreira D, Fortes A. Near surface mounted CFRP-based technique for the strengthening of concrete structures. Concrete 2004:1–13.

[20] Ceroni F. Experimental performances of RC beams strengthened with FRP materials. Constr Build Mater 2010;24:1547–59. https://doi.org/10.1016/j.conbuildmat.2010.03.008.

[21] Soliman SM, El-Salakawy E, Benmokrane B. Flexural behaviour of concrete beams strengthened with near surface mounted fibre reinforced polymer bars. Can J Civ Eng 2010;37:1371–82. https://doi.org/10.1139/L10-077.

[22] Barris C, Sala P, Gómez J, Torres L. Flexural behaviour of FRP reinforced concrete beams strengthened with NSM CFRP strips. Compos Struct 2020;241:112059. https://doi.org/10.1016/j.compstruct.2020.112059.

[23] Lee S, Lee C. Prediction of shear strength of FRP-reinforced concrete flexural members without stirrups using artificial neural networks. Eng Struct 2014;61:99–112. https://doi.org/10.1016/j.engstruct.2014.01.001.

[24] Naderpour H, Poursaeidi O, Ahmadi M. Shear resistance prediction of concrete beams reinforced by FRP bars using artificial neural networks. Measurement 2018;126:299–308. https://doi.org/10.1016/j.measurement.2018.05.051.

[25] Cortez P, Embrechts MJ. Using sensitivity analysis and visualization techniques to open black box data mining models. Inf Sci (Ny) 2013;225:1–17. https://doi.org/10.1016/j.ins.2012.10.039.

[26] Ghanizadeh AR, Ghanizadeh A, Asteris PG, Fakharian P, Armaghani DJ. Developing bearing capacity model for geogrid-reinforced stone columns improved soft clay utilizing MARS-EBS hybrid method. Transp Geotech 2023;38:100906. https://doi.org/10.1016/j.trgeo.2022.100906.

[27] Chen L, Fakharian P, Rezazadeh Eidgahee D, Haji M, Mohammad Alizadeh Arab A, Nouri Y. Axial compressive strength predictive models for recycled aggregate concrete filled circular steel tube columns using ANN, GEP, and MLR. J Build Eng 2023;77:107439. https://doi.org/10.1016/j.jobe.2023.107439.

[28] Chen Q, Norcio AF, Wang J. Neural Network Based Stereotyping for User Profiles. Neural Comput Appl 2000;9:259–65. https://doi.org/10.1007/s005210070003.

[29] Naderpour H, Haji M, Mirrashid M. Shear capacity estimation of FRP-reinforced concrete beams using computational intelligence. Structures 2020;28:321–8. https://doi.org/10.1016/j.istruc.2020.08.076.

[30] Naderpour H, Kheyroddin A, Amiri GG. Prediction of FRP-confined compressive strength of concrete using artificial neural networks. Compos Struct 2010;92:2817–29. https://doi.org/10.1016/j.compstruct.2010.04.008.

[31] Naderpour H, Alavi SA. A proposed model to estimate shear contribution of FRP in strengthened RC beams in terms of Adaptive Neuro-Fuzzy Inference System. Compos Struct 2017;170:215–27. https://doi.org/10.1016/j.compstruct.2017.03.028.

[32] Naderpour H, Rafiean AH, Fakharian P. Compressive strength prediction of environmentally friendly concrete using artificial neural networks. J Build Eng 2018;16:213–9. https://doi.org/10.1016/j.jobe.2018.01.007.

[33] Fakharian P, Rezazadeh Eidgahee D, Akbari M, Jahangir H, Ali Taeb A. Compressive strength prediction of hollow concrete masonry blocks using artificial intelligence algorithms. Structures 2023;47:1790–802. https://doi.org/10.1016/j.istruc.2022.12.007.

[34] Mehany S, Mohamed HM, Benmokrane B. Flexural Behavior and Serviceability Performance of Lightweight Self-Consolidating Concrete Beams Reinforced with Basalt Fiber-Reinforced Polymer Bars. ACI Struct J 2023;120:47–60. https://doi.org/10.14359/51738502.

[35] Uzdil O, Sayın B, Coşgun T. Examination of parameters impacting flexural and shear strengthening of RC beams. J Struct Eng Appl Mech 2022;5:117–34. https://doi.org/10.31462/jseam.2022.03117134.

[36] Askar MK, Hassan AF, Al-Kamaki YSS. Flexural and shear strengthening of reinforced concrete beams using FRP composites: A state of the art. Case Stud Constr Mater 2022;17:e01189. https://doi.org/10.1016/j.cscm.2022.e01189.

[37] Al-Obaidi S, Saeed YM, Rad FN. Flexural strengthening of reinforced concrete beams with NSM-CFRP bars using mechanical interlocking. J Build Eng 2020;31:101422. https://doi.org/10.1016/j.jobe.2020.101422.

[38] Panahi M, Zareei SA, Izadi A. Flexural strengthening of reinforced concrete beams through externally bonded FRP sheets and near surface mounted FRP bars. Case Stud Constr Mater 2021;15:e00601. https://doi.org/10.1016/j.cscm.2021.e00601.

[39] Suliman AKS, Jia Y, Mohammed AAA. Experimental evaluation of factors affecting the behaviour of reinforced concrete beams strengthened by NSM CFRP strips. Structures 2021;32:632–40. https://doi.org/10.1016/j.istruc.2021.03.058.

[40] Al-Abdwais AH, Al-Mahaidi RS. Experimental and finite element analysis of flexural performance of RC beams retrofitted using near-surface mounted with CFRP composites and cement adhesive. Eng Struct 2021;241:112429. https://doi.org/10.1016/j.engstruct.2021.112429.

[41] Jahani Y, Baena M, Gómez J, Barris C, Torres L. Experimental Study of the Effect of High Service Temperature on the Flexural Performance of Near-Surface Mounted (NSM) Carbon Fiber-Reinforced Polymer (CFRP)-Strengthened Concrete Beams. Polymers (Basel) 2021;13:920. https://doi.org/10.3390/polym13060920.

[42] Murad Y, Abu-AlHaj T. Flexural strengthening and repairing of heat damaged RC beams using continuous near-surface mounted CFRP ropes. Structures 2021;33:451–62. https://doi.org/10.1016/j.istruc.2021.04.079.

[43] Abdallah M, Al Mahmoud F, Khelil A, Mercier J, Almassri B. Assessment of the flexural behavior of continuous RC beams strengthened with NSM-FRP bars, experimental and analytical study. Compos Struct 2020;242:112127. https://doi.org/10.1016/j.compstruct.2020.112127.

[44] Imjai T, Setkit M, Garcia R, Figueiredo FP. Strengthening of damaged low strength concrete beams using PTMS or NSM techniques. Case Stud Constr Mater 2020;13:e00403. https://doi.org/10.1016/j.cscm.2020.e00403.

[45] Yazdani N, Aljaafreh T, Beneberu E. Concrete beam flexural strengthening with anchored pre-saturated CFRP laminates. Compos Struct 2020;235:111733. https://doi.org/10.1016/j.compstruct.2019.111733.

[46] Abdelkarim OI, Ahmed EA, Mohamed HM, Benmokrane B. Flexural strength and serviceability evaluation of concrete beams reinforced with deformed GFRP bars. Eng Struct 2019;186:282–96. https://doi.org/10.1016/j.engstruct.2019.02.024.

[47] Obaidat YT, Ashteyat AM, Obaidat AT. Performance of RC Beam Strengthened with NSM-CFRP Strip Under Pure Torsion: Experimental and Numerical Study. Int J Civ Eng 2020;18:585–93. https://doi.org/10.1007/s40999-019-00487-2.

[48] Panahi M, Izadinia M. A Parametric Study on the Flexural Strengthening of Reinforced Concrete Beams with Near Surface Mounted FRP Bars. Civ Eng J 2018;4:1917. https://doi.org/10.28991/cej-03091126.

[49] Sharaky IA, Baena M, Barris C, Sallam HEM, Torres L. Effect of axial stiffness of NSM FRP reinforcement and concrete cover confinement on flexural behaviour of strengthened RC beams: Experimental and numerical study. Eng Struct 2018;173:987–1001. https://doi.org/10.1016/j.engstruct.2018.07.062.

[50] Yaseen SA. Flexural Behavior of Self Compacting Concrete T-Beams Reinforced with AFRP. Eurasian J Sci Eng 2018;4. https://doi.org/10.23918/eajse.v4i2p178.

[51] Daghash SM, Ozbulut OE. Flexural performance evaluation of NSM basalt FRP-strengthened concrete beams using digital image correlation system. Compos Struct 2017;176:748–56. https://doi.org/10.1016/j.compstruct.2017.06.021.

[52] Haddad RH, Almomani OA. Recovering flexural performance of thermally damaged concrete beams using NSM CFRP strips. Constr Build Mater 2017;154:632–43. https://doi.org/10.1016/j.conbuildmat.2017.07.211.

[53] Al-Saadi NTK, Mohammed A, Al-Mahaidi R. Performance of RC beams rehabilitated with NSM CFRP strips using innovative high-strength self-compacting cementitious adhesive (IHSSC-CA) made with graphene oxide. Compos Struct 2017;160:392–407. https://doi.org/10.1016/j.compstruct.2016.10.084.

[54] Goldston MW, Remennikov A, Sheikh MN. Flexural behaviour of GFRP reinforced high strength and ultra high strength concrete beams. Constr Build Mater 2017;131:606–17. https://doi.org/10.1016/j.conbuildmat.2016.11.094.

[55] Khalifa AM. Flexural performance of RC beams strengthened with near surface mounted CFRP strips. Alexandria Eng J 2016;55:1497–505. https://doi.org/10.1016/j.aej.2016.01.033.

[56] Mahal M, Täljsten B, Blanksvärd T. Experimental performance of RC beams strengthened with FRP materials under monotonic and fatigue loads. Constr Build Mater 2016;122:126–39. https://doi.org/10.1016/j.conbuildmat.2016.06.060.

[57] Yang JM, Min KH, Shin HO, Yoon YS. Behavior of High-Strength Concrete Beams Reinforced with Different Types of Flexural Reinforcement and Fiber. Adv. FRP Compos. Civ. Eng., vol. L, Berlin, Heidelberg: Springer Berlin Heidelberg; 2011, p. 275–8. https://doi.org/10.1007/978-3-642-17487-2_58.

[58] Nurbaiah MN, Hanizah AH, Nursafarina A, Nur Ashikin M. Flexural behaviour of RC beams strengthened With externally bonded (EB) FRP sheets or Near Surface Mounted (NSM) FRP rods method. 2010 Int. Conf. Sci. Soc. Res. (CSSR 2010), IEEE; 2010, p. 1232–7. https://doi.org/10.1109/CSSR.2010.5773725.

[59] Al-mahmoud F, Castel A, François R, Tourneur C. RC beams strengthened with NSM CFRP rods and modeling of peeling-off failure 2010;92:1920–30. https://doi.org/10.1016/j.compstruct.2010.01.002.

[60] Akbarzadeh H, Maghsoudi AA. Experimental and analytical investigation of reinforced high strength concrete continuous beams strengthened with fiber reinforced polymer. Mater Des 2010;31:1130–47. https://doi.org/10.1016/j.matdes.2009.09.041.

[61] Perera R, Vique J, Arteaga A, Diego A De. Shear capacity of reinforced concrete members strengthened in shear with FRP by using strut-and-tie models and genetic algorithms. Compos Part B Eng 2009;40:714–26. https://doi.org/10.1016/j.compositesb.2009.06.008.

[62] Wang B, Teng JG, Lorenzis L De, Zhou L, Ou J, Jin W, et al. Strain monitoring of RC members strengthened with smart NSM FRP bars. Constr Build Mater 2009;23:1698–711. https://doi.org/10.1016/j.conbuildmat.2008.07.027.

[63] Al-Mahmoud F, Castel A, François R, Tourneur C. Strengthening of RC members with near-surface mounted CFRP rods. Compos Struct 2009;91:138–47. https://doi.org/10.1016/j.compstruct.2009.04.040.

[64] Hashemi SH, Rahgozar R, Maghsoudi AA. Flexural testing of high strength reinforced concrete beams strengthened with CFRP sheets. Int J Eng Trans B Appl 2009;22:131–46.

[65] Barros JAO, Dias SJE, Lima JLT. Efficacy of CFRP-based techniques for the flexural and shear strengthening of concrete beams. Cem Concr Compos 2007;29:203–17. https://doi.org/10.1016/j.cemconcomp.2006.09.001.

[66] Hassan T, Rizkalla S. Investigation of Bond in Concrete Structures Strengthened with Near Surface Mounted Carbon Fiber Reinforced Polymer Strips. J Compos Constr 2003;7:248–57. https://doi.org/10.1061/(ASCE)1090-0268(2003)7:3(248).

[67] Jung WT, Park YH, Park JS, Kang JY, You YJ. Experimental investigation on flexural behavior of RC beams strengthened by NSM CFRP reinforcements. Am. Concr. Institute, ACI Spec. Publ., vol. SP-230, 2005, p. 795–805.

[68] Barros J, Kotynia R. Possibilities and challenges of NSM for the flexural strengthening of RC structures. Proc. 4th Int. Conf. FRP Compos. Civ. Eng. CICE 2008, 2008, p. 22–4.

[69] Soudki K, Alkhrdaji T. Guide for the Design and Construction of Externally Bonded FRP Systems for Strengthening Concrete Structures (ACI 440.2R-02). Struct. Congr. 2005, Reston, VA: American Society of Civil Engineers; 2005, p. 1–8. https://doi.org/10.1061/40753(171)159.